HNPS Advances in Nuclear Physics

Vol 28 (2021)

HNPS2021

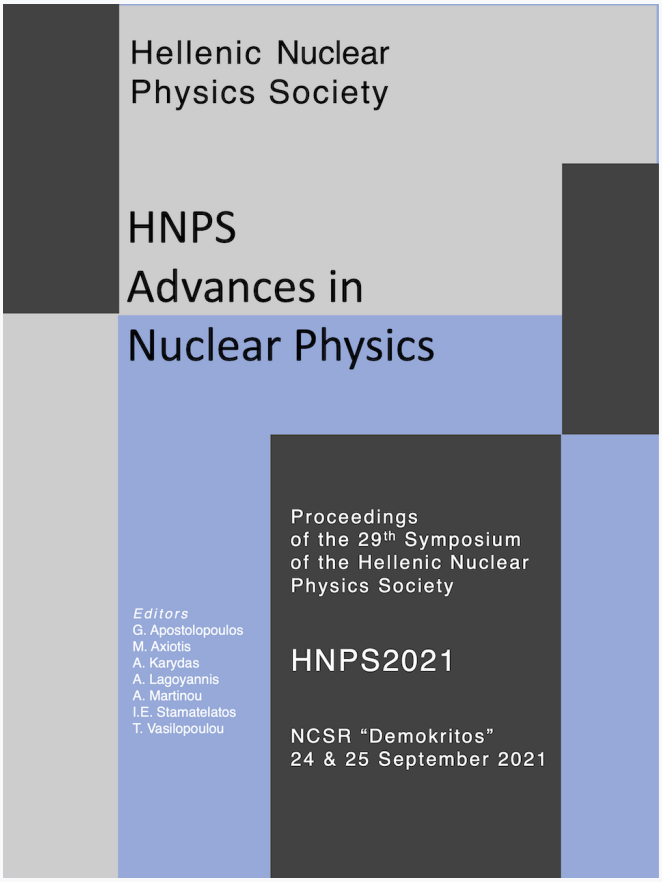

Spin distribution of the nuclear level density in a shell model approach

Luke Newman, Sofia Karampagia

doi: 10.12681/hnps.3614

To cite this article:

Newman, L., & Karampagia, S. (2022). Spin distribution of the nuclear level density in a shell model approach. *HNPS Advances in Nuclear Physics*, *28*, 123–128. https://doi.org/10.12681/hnps.3614

Spin distribution of the nuclear level density in a shell model approach

L. Newman[1], S. Karampagia[1,2,*]

[1] *Grand Valley State University, Allendale, MI, 49401-9403, USA*
[2] *NSCL/FRIB Michigan State University, East Lansing, Michigan 48824-1321, USA*

Abstract Nuclear level densities (NLDs) are key ingredients in calculations of neutron capture rates for neutron rich isotopes in nuclear astrophysics applications. Available experimental NLDs are limited mainly to nuclei near stability. Therefore, theoretical models are employed to predict the NLDs of neutron rich nuclei. Here we present a methodology for calculating spin- and parity- dependent NLDs using methods of statistical spectroscopy, based on the Shell Model. The spin distribution of the NLDs is predicted for nuclei in the *sd* and *pf* shells.

Keywords nuclear level densities, shell model, spin distribution

INTRODUCTION

The nuclear level density (NLD) is defined as the number of levels per energy bin at a certain excitation energy. The knowledge of the NLD is important for the theoretical prediction of the neutron capture rates for neutron rich isotopes, where the experimental determination of these rates is challenging. The uncertainties in NLD lead to significantly different predictions of neutron capture rates, even for nuclei with a few neutrons away from the stable isotope [1], which in turn leads to significantly different predictions of the isotopic abundance pattern [2].

Experimental nuclear level densities can be obtained either at low excitation energies by counting the experimentally available energy levels of complete nuclear energy spectra or at excitation energies equal to the particle separation energies. The latter, however, are available for limited spin values. Recently, an experimental technique which uses charged-particle reactions has been developed, that produces level densities in the intermediate statistical energy region, the Oslo method [3] and the beta-Oslo technique [4]. An alternate technique used for the deduction of level densities is the particle evaporation technique [5]. Despite these experimental efforts to derive NLDs, their availability is still scarce, and their knowledge relies heavily on theoretical models.

NLDs have been historically predicted using phenomenological models, such as the Fermi gas formula and the constant temperature formula [6]. These formulas have parameters which are determined by performing fits to the available experimental data. These models determine the total level density of a particular nuclear species and the spin dependent nuclear level density has to be derived by the formula

$$\rho(E,J) = f(J)\rho(E), \quad (1)$$

where $f(J)$ is the spin distribution and $\rho(E)$ is the total level density. Also available are Hartree-Fock-Bogolyubov NLDs which are spin and parity dependent [7]. The calculation of the NLDs starts from single-particle level calculations and then pairing and other collective

* Corresponding author: karampso@gvsu.edu

effects, such as rotational and vibrational enhancements are added. These have been incorporated in reaction codes, such as TALYS [8], and are therefore widely used for the calculation of reaction rates. A shell model approach used for NLD calculations is the Shell Model Monte Carlo method [9] which also provides spin and parity dependent NLDs. One drawback of this method is that the calculations are time consuming and cannot be performed for a large number of nuclei. Another approach that was recently developed is the Lanczos method [10], which also produces spin and parity dependent level densities. This approach produces NLDs which are very close to the NLDs derived with the configuration interaction shell model using a conventional diagonalization of the Hamiltonian. It requires a few iterations in the full shell model basis to give results, so it is not appropriate for shell model spaces with many valence nucleons. In this paper, for the calculation of level densities we will use the moments method [11], a method which is based on statistical spectroscopy [12]. The moments method uses the shell model spaces and interaction Hamiltonians of the configuration interaction shell model, but it does not require the diagonalization of the shell model Hamiltonian. It also produces spin and parity dependent nuclear level densities.

THE MOMENTS METHOD

Instead of calculating the eigenvalues, the moments method aims to the calculation of the distribution of the eigenvalues. The form of the distribution of the eigenvalues can be fully known if the moments of the Hamiltonian are known. To calculate the moments of the Hamiltonian and eventually the level density, the moments method implements partitions of particles. The partitions, p, are all the possible ways of distributing the valence particles in single particle orbitals. It is assumed that the level density of any given partition, for states with the same quantum numbers, i.e. spin J, isospin T_z and parity π, is given by a Gaussian distribution. This is supported by results obtained from the configuration interaction shell model using the conventional diagonalization of the Hamiltonian and by studies of statistical spectroscopy [13].

Finite range Gaussians are used, G_{ap}, where p is the partition and a is a set of quantum numbers common for the states belonging to the partition. The total level density for a specific set of quantum numbers a, $\rho(E;a)$, is calculated as

$$\rho(E;a) = \sum_{p} D_{ap} G_{ap}(E)$$

where D_{ap} is the total number of states (dimension) having this specific set of quantum numbers a in partition p. The knowledge of the ground state energy is required. The centroid and the dispersion of the Gaussian are given by the first and second moments, respectively [14]. The centroid is the mean energy value of the set of states with the same quantum numbers in this partition and can be found as

$$E_{ap} = \langle H_{ap} \rangle = \frac{1}{D_{ap}} Tr^{ap} H$$

The dispersion is the standard deviation of the Gaussian and can be found as

$$\sigma_{ap}^2 = \langle H^2 \rangle_{ap} - E_{ap}^2 = \frac{1}{D_{ap}} Tr^{ap} H^2 - E_{ap}^2.$$

The moments method level density has been extensively compared with the level density obtained by the exact diagonalization of the shell model Hamiltonian and with the level density from the available experimental levels [14-18].

THE SPIN DISTRIBUTION, RESULTS AND DISCUSSION

When the total (spin-independent) level density of a particular nuclear species is known, the spin dependent nuclear level density is derived by Eq. (1). The spin distribution used in the literature is given by the spin cut-off model [19]

$$f(J,\sigma) = e^{-\frac{J^2}{2\sigma^2}} - e^{-\frac{(J+1)^2}{2\sigma^2}} = \frac{2J+1}{2\sigma^2} e^{-\frac{J(J+1)}{2\sigma^2}}, \quad (2)$$

where the individual nucleon spins are assumed to couple at random, therefore the spin distribution is a Gaussian-like curve which depends on a single parameter σ, the spin cut-off parameter. The spin distribution of the level densities has been studied both experimentally [20- 22] and theoretically [23,24].

In this work we are systematically deriving the spin cut-off parameter σ for nuclei in the *sd* and *pf* shells by fitting Eq. (2) on the spin dependent level density derived by the moments method at different excitation energy intervals, as seen in Fig. 1.

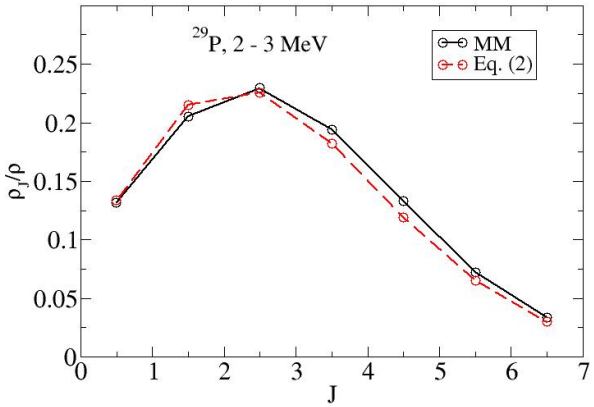

Fig. 1. *The spin distribution, $f(J) = \rho_J/\rho$, of energy levels of ^{29}P between 2 – 3 MeV, calculated with the moments method (black curve) along with the fitted line provided by Eq. (2) (red dashed curve).*

For the moments method calculation, we used the *sd* valence space, comprising of the $1s_{1/2}$, $0d_{3/2}$, $0d_{5/2}$ orbitals, assuming an inert ^{16}O core and the *pf* valence space, comprising of the $1p_{1/2}$, $1p_{3/2}$, $0f_{5/2}$, $0f_{7/2}$ orbitals, with ^{40}Ca as the inert core. We used the USDB [25] and GX1A [26] shell model interactions for the *sd* and *pf* model spaces, respectively. The spin distribution, $f(J)$, was derived for all *sd* and *pf* nuclei with at least 2 valence particles/holes in each model space. The spin distribution was derived in energy intervals of 1 MeV, starting from 2 – 3 MeV and going up 10 MeV for *sd* nuclei and 12 MeV for *pf* nuclei. We divided the nuclei in two groups; even-even nuclei and odd-odd, odd-even nuclei, and we studied separately the evolution of the spin cut-off parameter as a function of excitation energy for odd-odd and odd-even nuclei.

Contrary to odd-odd and odd-even nuclei whose calculated spin distribution follows the smooth Gaussian-like spin distribution of Eq. (2), the calculated spin distribution of even-even nuclei shows a characteristic odd-even staggering pattern. This staggering pattern was also observed in experimental data of even-even nuclei [21] and in Shell Model Monte Carlo calculations [23]. In [21] the authors used the following formula to describe the odd-even staggering pattern, $f_{ee}(J) = f(J,\sigma)(1+x)$, where x takes either positive or negative values. They found that independent of mass, the x parameter takes a single value for all even spin values, and a single value for all odd spin values. Zero spin levels must also be treated separately from even spin values, as they have significantly enhanced spin distribution compared to the rest of the even spin values. We used the same formula to derive the values for x for even-even nuclei and the resulting spin distribution of the even-even nucleus ^{56}Fe derived from the moments method is compared to the spin distribution from experimental data [21] and Shell Model Monte Carlo (SMMC) calculations [23] in Fig. 2. Also in Fig. 2, left panel, the spin distribution of the odd-even isotope ^{55}Fe is seen, which follows the Gaussian shape of the spin cut-off model both for experimental data and theoretical calculations

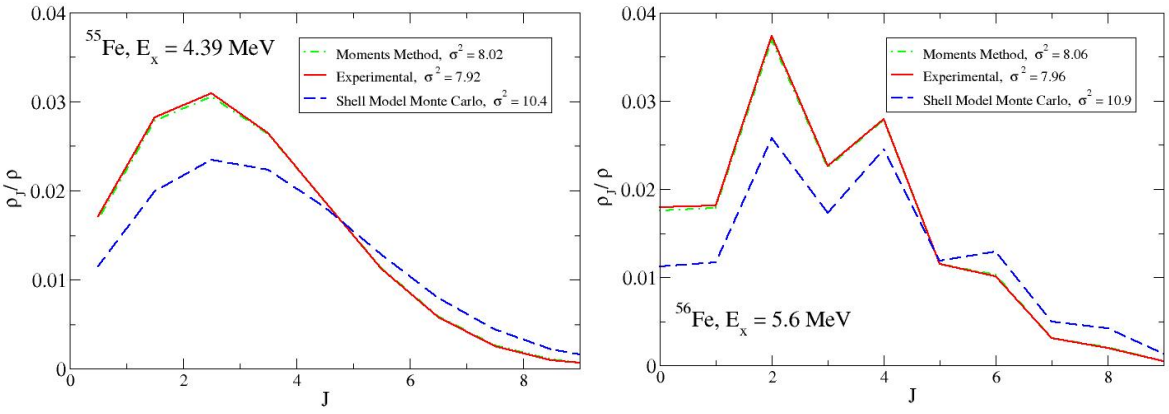

Fig. 2. *The spin distribution, $f(J) = \rho_J/\rho$, of ^{55}Fe (left panel), ^{56}Fe (right panel) at excitation energy 4.39 MeV and 5.6 MeV, respectively. The green dot-dash line is the spin distribution derived from moments method calculations, the red solid line is the spin distribution from experimental data and the blue dashed line is the spin distribution from Shell Model Monte Carlo calculations.*

The evolution of the spin cut-off parameter as a function of excitation energy and mass number for odd-odd, odd-even nuclei of the *sd* (left panel) and *pf* (right panel) model spaces is seen in Fig. 3. The lowest curve represents the 2 – 3 MeV energy interval and as the excitation energy increases, the spin cut-off parameter curve is also raised. The higher spin cut-off parameter curve represents the 9 – 10 MeV energy interval for *sd* nuclei and 11 – 12 MeV energy interval for *pf* nuclei.

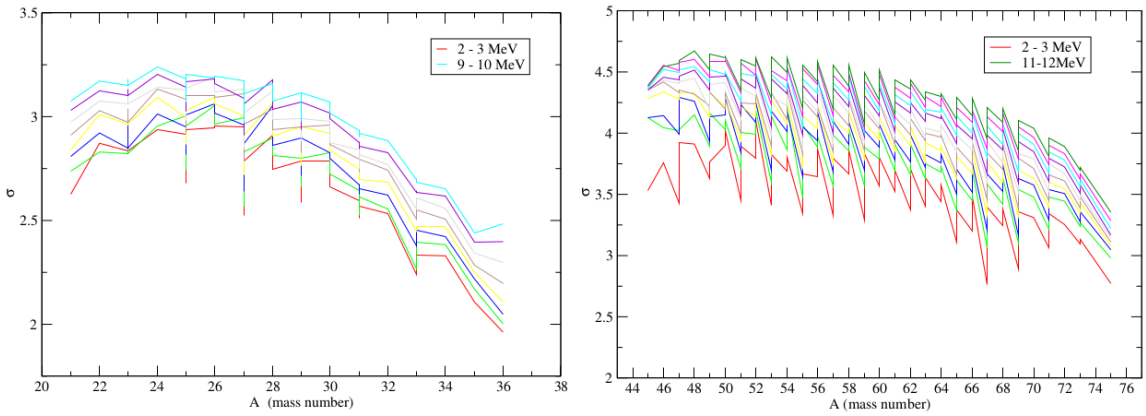

Fig. 3. *The spin cut-off parameter as a function of excitation energy and mass number for odd-odd, odd-even nuclei of the sd (left panel) and pf (right panel) model spaces. The lowest curve represents the spin cut-off parameter at the 2 – 3 MeV energy interval and the highest curve the spin cut-off parameter at the 9 – 10 MeV energy interval or 11 – 12 MeV energy interval for sd and pf nuclei, respectively.*

CONCLUSIONS

The spin distribution has been calculated using the moments method and the values of the spin cut-off parameter have been derived by fitting Eq. (2) to the calculated spin distribution. The fitting of Eq. (2) on the spin distributions of odd-odd and odd-even nuclei is excellent. We found that Eq. (2) cannot describe all spin values of even-even nuclei and an additional parameter has to be introduced to derive the spin cut-off parameter for even and odd values of spin. The moments method spin distribution in Fig. 2 is in excellent agreement with the spin distribution derived from experimental data. The spin distribution derived from SMMC calculations gives a higher spin cut-off parameter compared to the other two curves. The SMMC calculations are performed in the $pfg_{9/2}$ model space, which could explain the discrepancy with the moments method calculations. Additional calculations with the moments method, in the same model space should be performed to study the discrepancy. In [21], the authors attributed the discrepancy between the derived experimental and SMMC spin cut-off parameters to the higher excitation energy considered for the SMMC calculations (4.39 MeV for ^{55}Fe, 5.6 MeV for ^{56}Fe), compared to the experimental excitation energy (in [21] the excitation energies considered are usually below 3 MeV). Indeed, as seen in Fig. 3 the spin cut-off parameter increases with excitation energy. However, the authors of [21] do not mention what was the maximum experimental excitation energy considered specifically for ^{55}Fe, ^{56}Fe. Our calculations consider excitation energies up to 4 MeV and 5 MeV for ^{55}Fe, ^{56}Fe, respectively. If the experimental excitation energies indeed do not exceed the 3 MeV, then the moments method cut-off parameter should have been around 10% and 20% larger compared to the experimental cut-off parameter for ^{55}Fe, ^{56}Fe, respectively, in order to have agreement with the experimental results. The moments method results also indicate dependence of the spin cut-off parameter on mass number (Fig. 3), besides the dependence on excitation energy. Any theoretical expression derived for the spin cut-off parameter must therefore include both dependencies.

References

[1] S. N. Liddick et al., Phys. Rev. Lett. 116, p. 242502 (2016)
[2] M. R. Mumpower, et al., Prog. Part. Nucl. Phys. 86, p. 86 (2016)
[3] A Schiller et al., Nucl. Instr. Meth. Phys. Res. A 447, p. 498 (2000)
[4] A. Spyrou et al., Phys. Rev. Lett. 113, p. 232502 (2014)
[5] A. Wallner et al., Phys. Rev. C 51, p. 614 (1995)
[6] A. Gilbert et al., Can. J. Phys. 43, p. 1446 (1965)
[7] S. Goriely et al., PRC 78, p. 064307 (2008)
[8] A. J. Koning et al., Nucl. Dat. Sh., 113, p. 2841 (2012)
[9] Y. Alhassid et al., Phys. Rev. Lett. 99, p. 162504 (2007)
[10] W. E. Ormand et al., Phys. Rev. C 102, p. 014315 (2020)
[11] R. Sen'kov et al., Phys. Rev. C 93, p. 064304 (2016)
[12] S. S. M. Wong, Nuclear Statistical Spectroscopy (Oxford University Press, New York, 1986)
[13] S. S. M. Wong, Rev. Mod. Phys. 55, p. 385 (1981)
[14] R. A. Sen'kov et al., Comp. Phys. Comm. 184, p. 215 (2013)
[15] R. A. Sen'kov et al., Phys. Rev. C 82, p. 024304 (2010)
[16] M. Scott et al., NIC X, Proc. Sc. 053, p. 132, (2008)
[17] S. Karampagia et al., Atom. D. Nucl. D. Tab. 1, p. 120 (2017)
[18] S. Karampagia et al., Int. Jour. Mod. Phys. E29, p. 2030005 (2020)
[19] T. Ericson, Adv. Phys. 9, p. 425 (1960)
[20] S. M. Grimes, et al., Phys. Rev. C 18, p. 1100 (1978)
[21] T. von Egidy, et al., Phys. Rev. C 78, p. 051301(R) (2008)
[22] T. von Egidy, et al., Phys. Rev. C 80, p. 054310 (2009)
[23] Y. Alhassid, et al., Phys. Rev. Lett. 99, p. 162504 (2007)
[24] W. M. Spinella, et al., Phys. Rev. C 90, p. 014315 (2014)
[25] B. A. Brown, et. al., Phys. Rev. C 74, p. 034315 (2006)
[26] M. Honma, et al., Phys. Rev. C 65, p. 061301 (R) (2002)